EFFECT OF MOX FUEL AND THE ENDF/B-VIII ON THE AP1000 NEUTRONIC PARAMETERS CALCULATIONS BY USING MCNP6

by

Sonia M. REDA [1,2*], ***Ibrahim M. GOMAA*** [3], ***Ibrahim I. BASHTER*** [1], ***and Esmat A. AMIN*** [4]

[1] Physics Department, Faculty of Science, Zagazig University, Zagazig, Egypt
[2] Physics Department, College of Science, Jouf University, Sakaka, Saudi Arabia
[3] Zagazig Higher Institute for Engineering and Technology, Zagazig, Egypt
[4] Nuclear and Radiological Regulatory Authority, Cairo, Egypt

Scientific paper
https://doi.org/10.2298/NTRP190705002R

The present work studies the effect of introducing MOX fuel on Westinghouse AP1000 neutronic parameters. The neutronic calculations were performed by using the MCNP6 code with the ENDF/B-VII.1 library and the new release of the ENDF/B-VIII, the AP1000 core with three ^{235}U enrichment zones (2.35 %, 3.40 %, and 4.45 %). The obtained results showed that the simulated model for the AP1000 core satisfies the optimization criteria as a Westinghouse reference. The results which included: effective multiplication factor, k_{eff}, delayed neutron fraction, β_{eff}, excess reactivity, ρ_{ex}, shutdown margin, temperature reactivity coefficients, whole core depletion, neutron flux, power peaking factor and core power density, were calculated and compared with the available published results. The k_{eff} in the cold zero power was found to be 1.20495 and 1.20247 with the ENDF/B-VII.1 and the ENDF/B-VIII libraries, respectively, which matches the value of 1.205 presented in the AP1000 Design Control Document for the UO_2 fuel core. On the other hand, k_{eff} in the cold zero power was found to be 1.19988 and 1.19860 for MOX core with the ENDF/B-VII.1 and the ENDF/B-VIII libraries, respectively, which show good reception and confirm the safety of the design and efficient modeling of AP1000 reactor core.

Key words: AP1000 reactor, MOX fuel, neutronic parameters, MCNP6, ENDF/B-VIII

INTRODUCTION

Pressurized water reactors (PWR) constitute the large majority of world nuclear power plants and are one of the three types of light water reactors (LWR), the other types being boiling water reactors (BWR) and supercritical water reactors (SCWR) [1]. Egypt is currently building a nuclear power project in Addabaa. This project utilizes the pressurized water reactor technology of Russian origin. Therefore, it is important to acquire experience in evaluating PWR neutronic performance. The AP1000 is a two-loop 1000 MWe PWR, and it is an updated version of AP600. Passive safety systems are used to provide significant and measurable improvements in plant simplification, safety, reliability, investment protection and plant costs. The AP1000 uses mastered and proven technology, which is based on over 35 years of PWR operating experience around the world [2].

The AP1000 reactor core is a 17×17 typical assembly that uses Zirlo as cladding, (see fig. 1 and tab. 1. The core has 157 fuel assemblies, each having 264 fuel rods, 24 control rod guide tubes and a neutron monitor guide tube (see figs. 2 and 3).The fuel assemblies are arranged in a pattern forming approximately a right circular cylinder. Fuel assemblies of three different enrichments 2.35 %, 3.40 %, and 4.45 % were used in the initial core loading [3]. Reactivity is controlled by the movement of control rod assemblies and by changing the boric acid concentration in the coolant [4].

The feasibility of MOX fuel utilization in PWR has been demonstrated in nuclear power plants such as the AP1000 reactor. Fetterman [5] studied the AP1000 core design with 50 % of MOX loading. The purpose was to demonstrate that the AP1000 is able to meet the European requirement for MOX utilization without any reactor design changes. A 100 % UO_2 core design was compared with a mixed MOX/UO_2 core design. The reactivity, power and fuel performance results were discussed. The AP1000 was able to meet the Eu-

* Corresponding author; e-mail: sonreda@yahoo.com

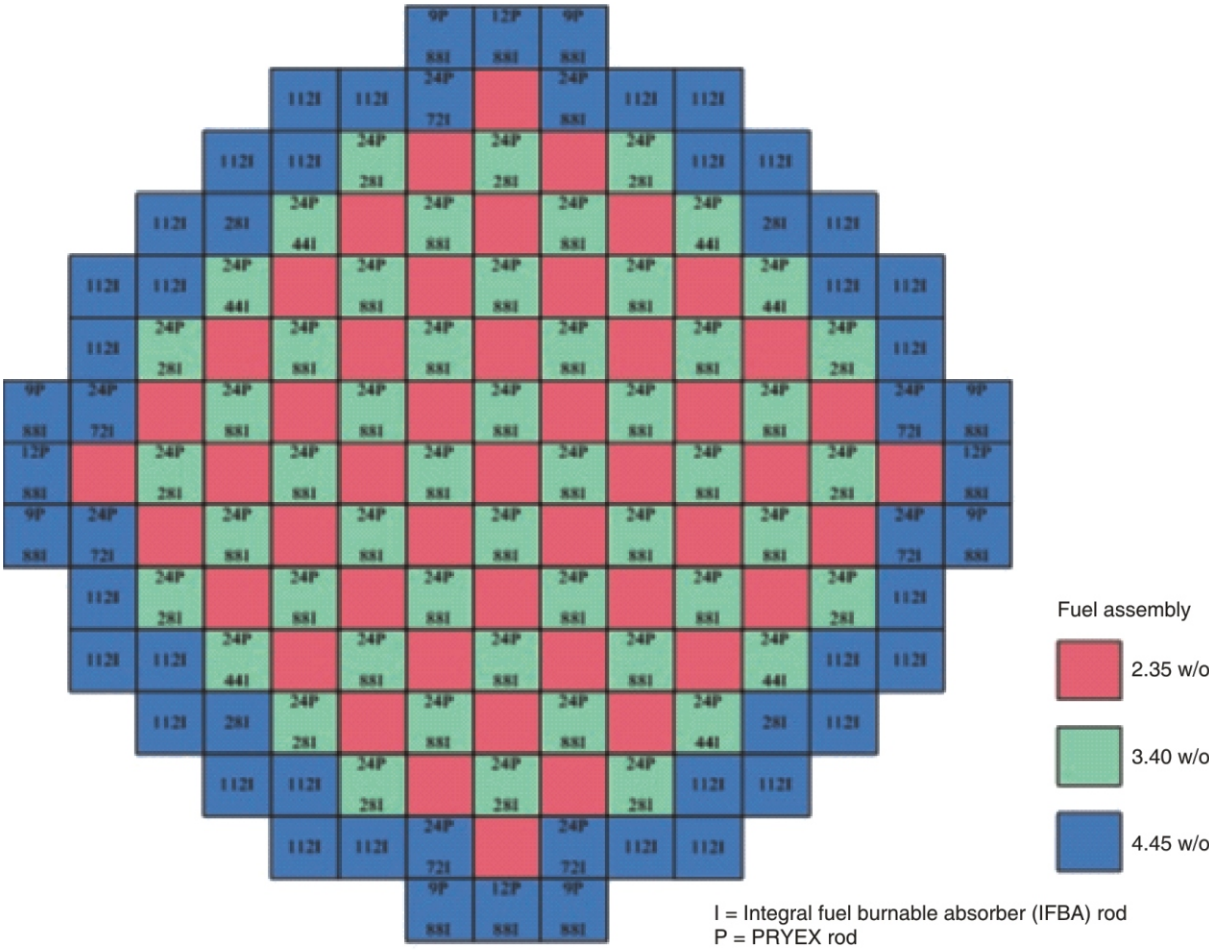

Figure 1. The AP1000 reactor core configuration [7]

Table 1. AP1000 rector core parameters [4]

Parameters	Value
Core configuration	
Active core equivalent diameter	304.038 cm
Active fuel height first core, cold	426 cm
Fuel assembly	
Total fuel assemblies	157
Rod array	17 17
Rods per assembly	264
Rod pitch	1.26 cm
Total power	3400 MWth
Fuel rod	
Outer diameter	0.94996 cm
Gab thickness	0.0165 cm
Clad thickness	0.0572 cm
Clad material	ZIRLO™
Clad density	6.5 gcm^{-3}
Material	UO_2 sintered
Density (% of theoretical)	95.5 %
Enrichment of UO_2	
Region 1	2.35 %
Region 2	3.40 %
Region 3	4.45 %
Diameter	0.8192 cm
Length of fuel pellet	0.98298 cm
Density of UO_2	10.4 gcm^{-3}

ropean requirement for the next generation of European passive plants and core designs with 100 % UO_2 and with MOX loadings of up to 50 %.

Washington and King [6] studied the ability of the AP1000 reactor in plutonium and minor actinide transmutation with a genetic search algorithm. The study objective was to use light water reactors in plutonium and minor actinide transmutation. The SCALE 6.1 and DAKOTA coupled model was used in three stages. The neutronic calculations for the AP1000 were evaluated for transmutation plutonium and minor actinides.

The purpose of this paper is to determine and present the neutronic parameters of the Westinghouse AP1000 reactor, and in addition to demonstrate that the AP1000 is capable of complying with MOX fuel utilization without significant changes in the design of the plant. The reactor parameters included criticality, power peaking factor, excess reactivity, boron concentration and total shutdown reactivity. Neutronic calculations were performed by MCNP6 code with ENDF/B-VII.1 and the newly released ENDF/B-VIII.

Current practice uses MOX fuel typically for a fraction of 30-50 % of the total core, while the rest of the core consists of conventional UO_2 assemblies. This strategy avoids some technological limitations that would affect 100 % MOX-loaded cores in current

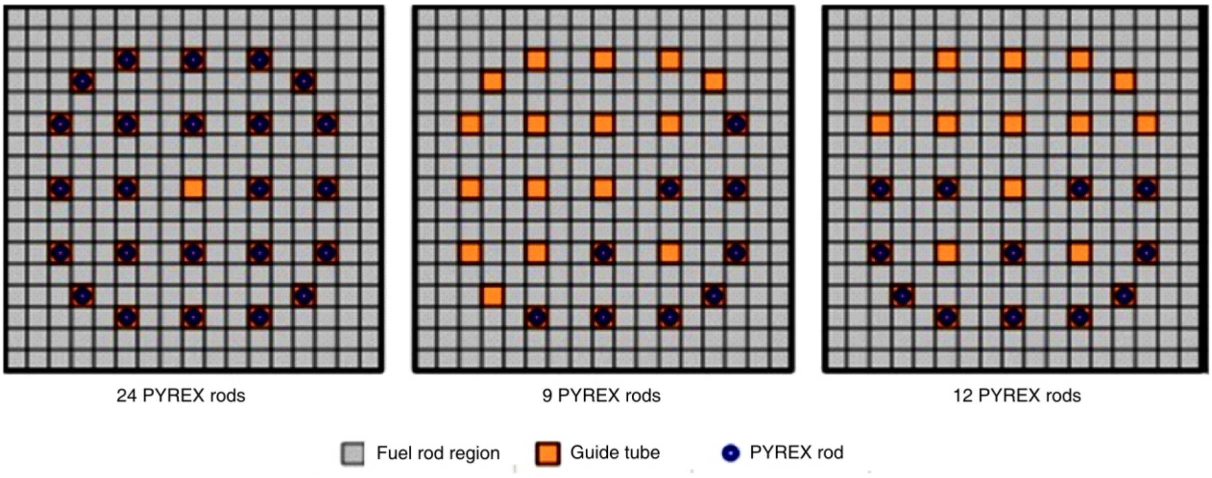

Figure 2. Arrangement of the PYREX ods in the fuel assembly [7]

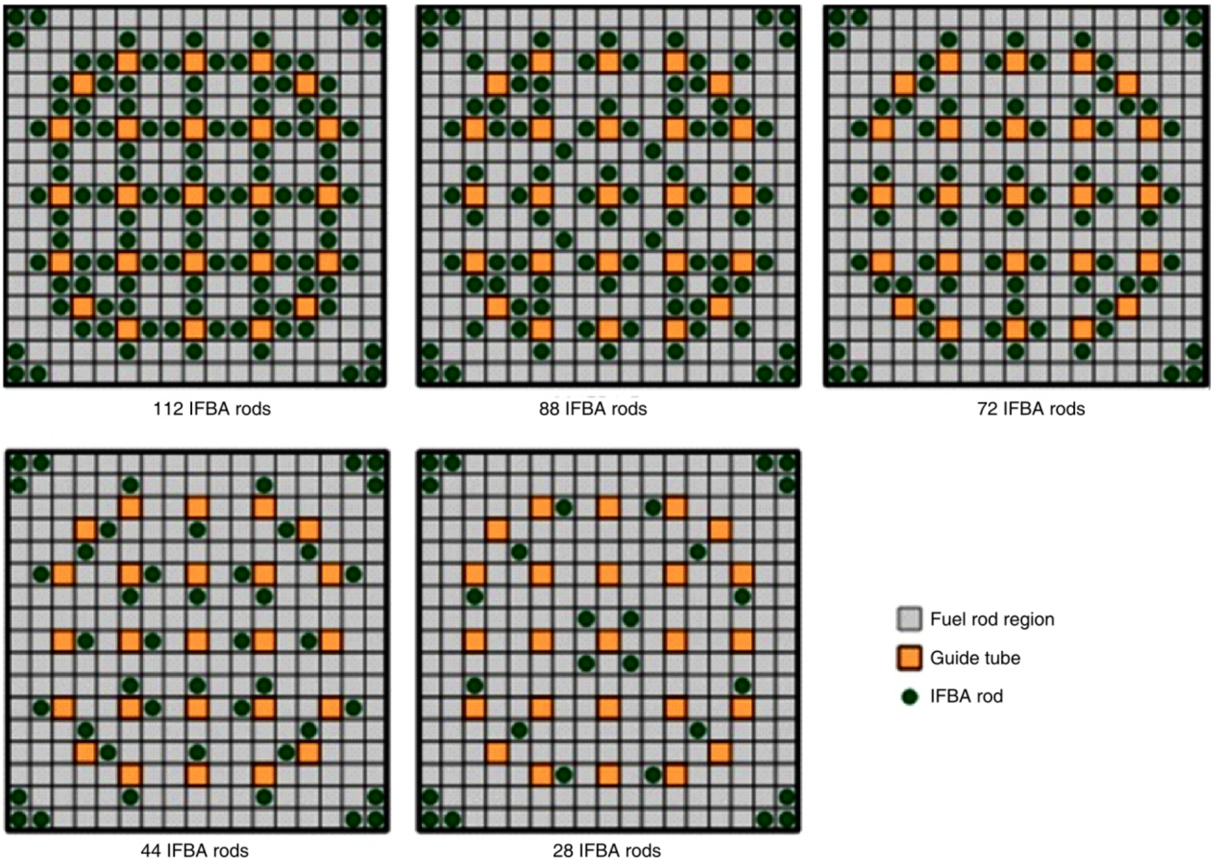

Figure 3. Arrangement of the IFBA rods in the fuel assembly [7]

LWR, since none of them have been designed for this specific purpose [8]. In order to meet these requirements, all the fuel assembles of regions 2 and 3 were not changed since they contain Pyrex and IFBA rods arrangements. The 48 fuel assemblies from region 1 with the enrichment of 2.35 % were replaced by MOX assemblies as in fig. 4, since they have not any Pyrex or IFBA rod arrangements; this was the best configuration without having to change the fuel assembly design variables and keeping the effective multiplication factor value below 1.205 as stated in the Westinghouse reference [4].

The plutonium isotopic composition depends on the reactor type and burnups of the reprocessed fuel. Fuel designers adopted two factors: the plutonium equivalence formulation and the consideration of the fissile plutonium content to enable the correct choice of the plutonium contents and the MOX fuel batch and to avoid deterioration of fuel quality. For LWR fuel and in a PWR 2 % ^{239}Pu in the plutonium isotopic com-

Nuclear Technology & Radiation Protection: Year 2019, Vol. 34, No. 4, pp. 325-335

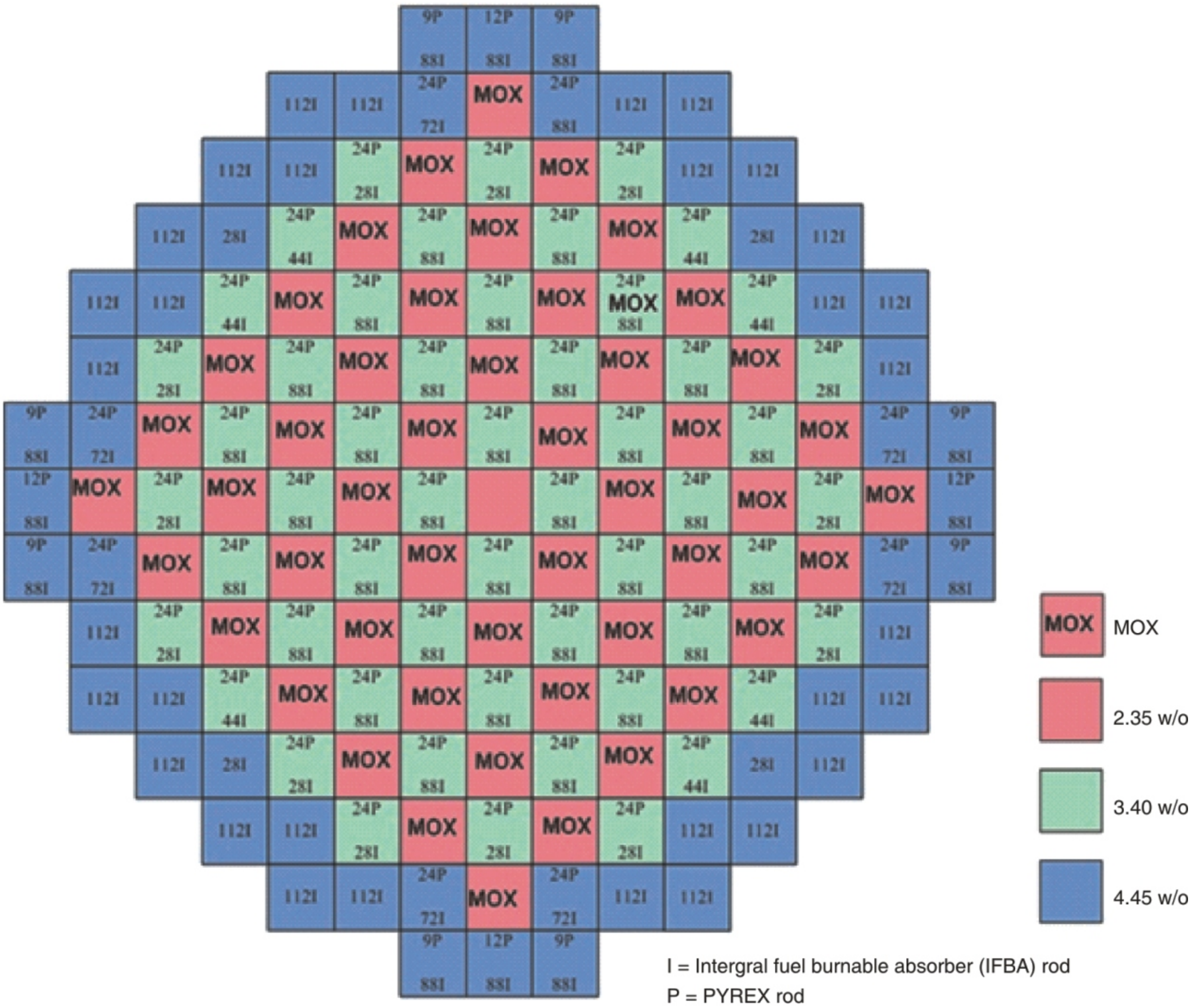

Figure 4. The MOX core configuration

Table 2. The MOX fuel isotopic composition

^{235}U	$3.8879\ 10^{-5}$	^{240}Pu	$9.9154\ \ ^{-4}$	^{16}O	$4.6330\ 10^{-2}$
^{238}U	$1.9159\ \ 0^{-2}$	^{241}Pu	$3.6732\ \ ^{-4}$		
^{238}Pu	$8.3986\ 10^{-5}$	^{241}Am	$1.0664\ 10^{-4}$		
^{239}Pu	$2.1706\ \ ^{-3}$	^{242}Am	$2.5174\ 10^{-4}$		

position is suggested to avoid power peaking since 2 % ^{239}Pu produces 6 % power peaking factor [9]. In order to keep these requirements the MOX fuel used in this simulation was with 2 % fissile ^{239}Pu and the percent of MOX fuel was 30.57 % of the total core. The MOX and plutonium isotopic compositions used in this simulation are presented in tab. 2.

MATERIAL AND METHOD

A 3-D model was designed to simulate the reactor neutronic parameters and compare UO_2 fuel and MOX fuel. The simulation was performed with the latest Monte Carlo code version with MCNP6 [10] by the ENDF/B-VII.1 and the ENDF/B-VIII cross-section libraries [11]. Table 3 shows the material compositions used in the simulation.

The ENDF/B-VIII cross section library has maximum changes for neutron reactions on nuclides including actinides which affect nuclear criticality simulations. Two of the most important re-evaluated isotopes are ^{235}U and ^{238}U. The re-evaluated parameters include the following:

Capture and fission cross-sections values

The capture cross-sections have been reduced when compared with the ENDF/B-VII.1 in the 0.5-2 keV region, but with increased energies up to 80 keV. The fission cross section evaluation corresponds to that in the ENDF/B-VII.1 with uncertainties that are around 0.4 % higher for incident energies that are below approximately 15 MeV.

Neutron multiplicity *v*

Neutron multiplicity *v* was re-evaluated and expanded below 30 eV to include fluctuations. Unlike the ENDF/B-VII.1 where *v* is constant over a wide

Table 3. Material compositions

Material	Isotope	Composition (mass fraction)	Material	Isotope	Composition (mass fraction)
UO_2(2.35w/o) 10.47 gcm^{-3}			ZrB_2 5.42 gcm^{-3}	5010	0.0187
	92235	5.56094375 10^{-4}		5011	0.1713
	92238	2.28162251 10^{-2}		40090	0.416745
	8016	4.67446389 10^{-2}		40091	0.090882
				40092	0.138915
				40094	0.140778
				40096	0.02268
UO_2 (3.40 w/o) 10.47 gcm^{-3}			PYREX 2.299 gcm^{-3}	5010	0.007
	92235	8.04549293 10^{-4}		5011	0.0319
	92238	2.23251989 10^{-2}		8016	0.5522
	8016	4.67501601 10^{-2}		14028	0.3772
				14029	0.0191
				14030	0.0126
UO_2(4.45 w/o) 10.47 gcm^{-3}	92235	1.0529963 10^{-3}	H_2O 1 gcm^{-3}	1001	0.111
	92238	2.2324844 10^{-2}		8016	0.889
	8016	4.6755681 10^{-2}			
He gap 0.0001604 gcm^{-3}	2003	0.00000137			
	2004	0.99999863			

range of incident neutron energy, the ENDF/B-VIII has not a constant v but its value varies as the incident neutron energy varies.

Thermal neutron constants

New evaluations of thermal neutron constants (TNC) show a neutron multiplicity reduction and a fission cross-section increment as compared with the ENDF/B-VII.1 evaluations at thermal energy, tab. 4 [12].

The (n, f) prompt fission neutron spectrum

The ENDF/B-VIII evaluation for the prompt fission neutron spectrum (PFNS) mean energy is clearly more flexible than that of the ENDF/B-VII.1, but fits well to experimental data. The new average released neutron energy became 2.00   0.01 MeV, and on the other hand it was 2.03 MeV in thermal range [13].

The (n, n') and (n, xn) cross sections

The ENDF/B-VIII evaluation for the total inelastic scattering cross-section (n, n') is slightly decreased than the last ENDF/B-VII.1 evaluation. The ENDF/BVIII evaluation for the (n, xn) secondary neutron wasn't changed, but showed a difference above 14 MeV [14].

Nubar

Evaluators use the parameter nubar to study criticality problems, since criticality is highly sensitive to nubar. A number of simulations have shown that the use of the new TNC and PFNS of the ENDF/B-VIII produce marginally higher k_{eff} values than that of the ENDF/B-VII.1 [14].

Table 4. The TNC values for the ENDF/B-VII.1, the ENDF/B-VIII and standards 2017

	B-VII.1	B-VIII.0	Standards 2017
σ_f (b*)	584.99	586.8	587.2(1.4)
σ (b)	98.69	99.4	99.3(2.0)
σ_{el} (b)	15.11	14.11	14.09(22)
v_{tot}	2.4367	2.4298	2.4250(50)
α	0.1687	0.1694	0.1690

*1b = 10^{-28}m^2

RESULTS AND DISCUSSIONS

The beginning of cycle

The first simulations were performed in cold conditions in order to determine the effective multiplication factor k_{eff}, the delayed neutron fraction β_{eff}, the excess reactivity ρ_{ex} and the shutdown margin (SDM). The results are shown in tab. 5.

The k_{eff} value was in a compatible range for UO_2 clean core (without control rods and chemical control). The AP1000 clean core was designed with initial k_{eff} = 1.205. The k_{eff} result showed good agreement with the AP1000 (DCD ([4] and the published data [15-17].

The k_{eff} value in MOX was slightly smaller than the obtained UO_2 results (1.20495 and 1.20247, respectively). The differences in the reactivity between the two types of fuel arose from different fissile material, which was ^{235}U in UO_2 while fissile materials

Table 5. The results of the beginning of cycle for UO_2 and MOX core

	Data source	k_{eff}	Relative error	β_{eff}	Relative error	ρ_{ex}	SDM %
UO_2	MCNP6 (ENDF/B-VII.1) (current result)	1.20495	0.00012	0.00676	0.00011	0.17009	4.92
	MCNP6 (ENDF/B-VIII) (current result)	1.20247	0.00046	0.00633	0.00017	0.168	–
	AP1000 (DCD) [4]	1.205	–	0.0075		0.17012	5.60
	WIMS9 [15]	1.2038	0.100	–		0.16929	–
	Serpent code [17]	1.20201	0.00051	–		0.16958	
	MCNP6 [19]	–	–	0.00695	0.00013	–	–
	MCNP6 (ENDF/B-VII.1)	1.19988	0.00018	0.00521	0.00019	0.1665	–
MOX	MCNP6 (ENDF/B-VIII)	1.19860	0.00014	0.0052	0.00013	0.165	–

Table 6. Temperature reactivity coefficients calculations

	Data source	$_{T,M}$ (pcm*/F)	DC (pcm/F)	α_{Total} (pcm/F)
UO_2	MCNP6 (ENDF/B-VII.1) (current result)	–11.0418	–1.4966	–12.5384
	MCNP6 (ENDF/B-VIII) (current result)	–8.28	–1.32	–9.6
	AP1000 (DCD) Design Limits [4]	0 to –40	–3.5 to –1.0	
	AP1000 (DCD) Best estimate [4]	0 to –35	–2.1 to –1.3	
MOX	MCNP6 (ENDF/B-VII.1)	–10.92	–0.903	–11.823
	MCNP6 (ENDF/B-VIII)	–9.083	–0.965	–10.048

*1 pcm = 10^{-5}

were ^{239}Pu and ^{241}Pu in MOX. The higher values of thermal fission and absorption cross-sections of ^{239}Pu resulted in lower thermal flux in MOX assemblies compared to UO_2 assemblies [18].

The β_{eff} values were 0.00676   0.00011 and 0.00633   0.00017 with the ENDF/B-VII.1 and the ENDF/B-VIII, respectively, for UO_2 fuel. The fraction of ^{235}U fission delayed neutron yields was calculated by Sembiring *et al*., [19] as 0.00695   0.00013 by using the ENDF/B-VII.1, while AP1000 design value was β_{eff} = 0.0075 [4]. The present results showed a good agreement with the published ones.

For MOX core, β_{eff} value is in a relatively acceptable range compared with that of UO_2 one (0.00521 and 0.00676 with the ENDF/B-VII.1, respectively, and 0.0052 and 0.00633 with the ENDF/B-VIII respectively). The ^{239}Pu had a delayed neutron fraction significantly smaller than ^{235}U and so MOX cores responded more quickly than UO_2 cores [18]. The ρ_{ex} value in UO_2 was very close to the AP1000 value (0.170124) and it was in good agreement with the other references. The shutdown margin calculated was 4.92 % which is in good agreement with Westinghouse reference (5.6 %). The ρ_{ex} value was within an acceptable range for MOX core as well.

One of the most important safety parameters of any nuclear reactor is how its reactivity responds to the change in temperature. This parameter is the temperature coefficient of reactivity and it should be negative, which means that as temperature increases, the reactivity should decrease [20]. The temperature coefficient of reactivity is divided into the moderator temperature coefficient $\alpha_{T,M}$ and the fuel temperature coefficient or doppler coefficient (DC). Their calculated values are shown in tab. 6.

For the AP1000 reactor, the $\alpha_{T,M}$ fell within the range of 0 to –40 pcm/F, while the DC fell within the range of –3.5 to –1.0 pcm/F. The most important consideration was that $\alpha_{T,M}$ and DC results obtained from this simulation agreed with those calculated in AP1000 Design Control Document [4] and were negative which meant that any increase in temperature resulted in a decrease in reactor reactivity and power [20]. The MOX fuel resulted in a slightly larger Doppler Coefficient and a significantly larger moderator temperature coefficient [18].

The middle of cycle

The MCNP6 was used to simulate the core performance over time. The behavior of k_{eff} over time for AP1000 core is shown in fig. 5. It is clear that keff is very consistent with referenced data [15-17]. Data in fig. 5 reveal that the reactor can operate 18 months with k_{eff} greater than the unity, which is confirmed in the AP1000 (DCD) [4]. The variation of Burnup with time for UO_2 and MOX cores with the ENDF/B-VII.1 is shown in fig. 6.

When comparing the fission cross-sections in the evaluated nuclear data files, the ENDF/B-VII.1 and the ENDF/B-VIII, one can find that the thermal fission cross section for ^{235}U differs by 1.81b (586.8 b in the ENDFB/B-VIII and 584.99b in the ENDF/B-VII.1). Moreover, the total neutron multiplicity ν was found to be greater with the ENDF/B-VIII (0.1694) than with the ENDF/B-VII.1 (0.1687), fig. 5. These differences may be the result of the increase in k_{eff} especially with the burn time in UO_2 fuel when using the ENDF/B-VIII [12, 14].

In relation to MOX fuel, the ENDF/B-VIII, ^{239}Pu prompt fission neutron spectrum (PFNS) comes from three different evaluations of Los Alamos. At thermal en-

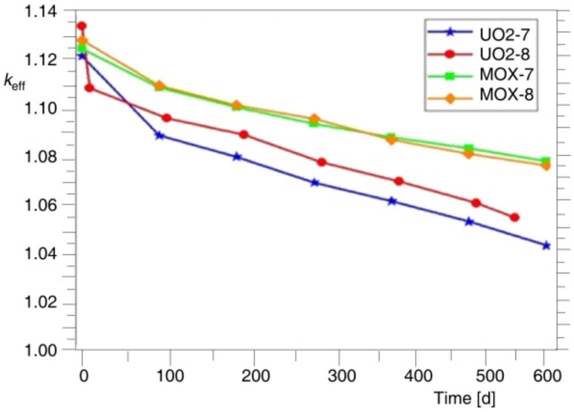

Figure 5. The k_{eff} variation with time for UO_2 and MOX cores

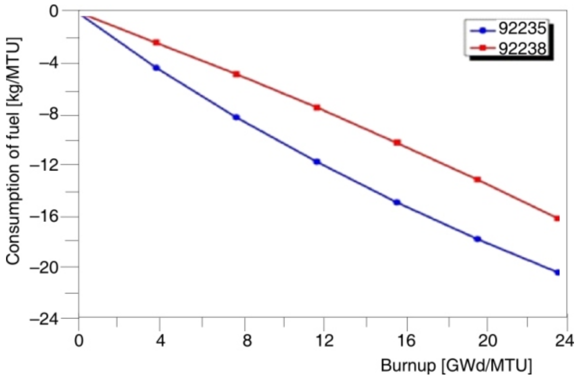

Figure 7. Consumption of fuel with burnup in UO_2 fuel

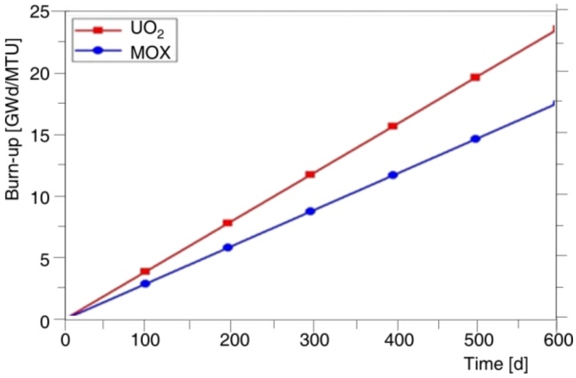

Figure 6. The variation of burnup with time for UO_2 and MOX cores

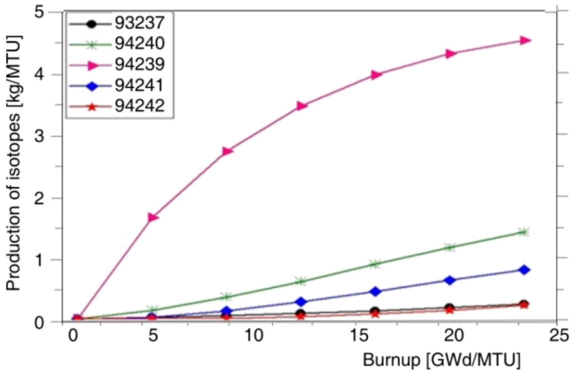

Figure 8. Production of Pu isotopes and other actinides with burnup in UO_2 fuel

ergies, the PFNS is a very slightly modified version of the ENDF/B-VII.1, so that its shape remains very similar to the original in the ENDF/B-VII.1 PFNS. Recent information which explains the discrepancies between the legacy of ^{239}Pu PFNS measurements was included in the new evaluation by increasing uncertainties. In conclusion, the results of ^{239}Pu were slightly different from the ENDF/B-VII.1 and the ENDF/B-VIII [14]. Because of the lower amount of ^{235}U in MOX fuel than in UO_2, the variation in k_{eff} was very small, fig. 5.

The end of cycle (EOC) of UO_2 fuel

The 2^{35}U is the fissionable material in the core which gradually decreases throughout core lifetime. Moreover, the production of ^{239}Pu and ^{241}Pu increases towards the EOC [13]. From startup until the EOC, the fissile component ^{235}U is depleted and other fissile components are produced when ^{238}U is transmuted to higher actinides, particularly ^{239}Pu and ^{241}Pu. Figures 6 and 7 present the consumption of the fuel and the production of Pu isotopes and other actinides that buildup in the core, respectively.

Results in figs. 7 and 8 show good agreement with the AP1000 (DCD) [4] and other calculated results [7, 16, 17]. As the burnup level rises, the amount of total fission products (FP) in the core increases. The FP are neutron absorbers and have a strong negative effect on the core's neutron economy as time passes.

To maintain constant power throughout core lifetime, flux must constantly change to compensate for isotopic transformations caused by neutron irradiation. The main competing factors in the process are the consumption/production of fissile nuclides, the depletion of burnable poisons and the accumulation of fission products in the core. At the BOC, the burnable poisons are at full strength, but as time evolves the powerful thermal neutron absorber ^{10}B is depleted and consequently less thermal neutrons are removed from the system [7].

The cumulative effect translates to an increase in neutron flux [7]; this effect can be seen clearly in fig. 9 which provides the profile of the average neutron flux in fuel elements. Figure 10 shows the power distribution for the AP1000 core in units of MW. The power was calculated by MCNP using the F4 tally, then the tally was normalized to the steady-state thermal power of a critical system by the scaling factor mentioned below. It can be seen that the power peaks are in the middle core assemblies for 2.35 % enrichment.

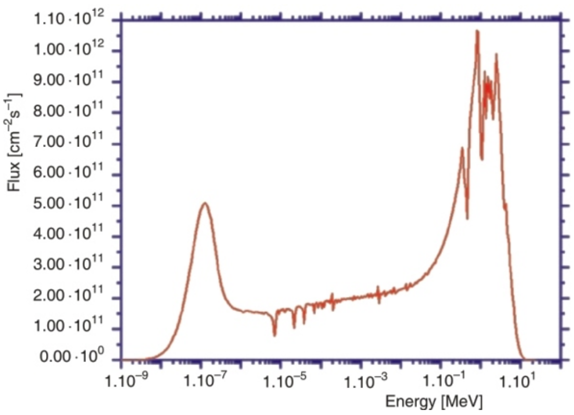

Figure 9. The AP1000 neutron flux with neutron energy

$$P \quad \frac{p[W]\nu \dfrac{\text{neutron}}{\text{fission}}}{1.6022\ \ 10^{\ 13}\ \dfrac{\text{J}}{\text{MeV}}\ \ W_f\ \dfrac{\text{MeV}}{\text{fission}}}\ \frac{1}{k_{\text{eff}}} F4$$

The end of cycle (EOC) of MOX fuel

The burnup results for MOX core are depicted in figs. 11-13. In the UO_2 core, the ^{235}U was the fissionable material which was gradually depleted with time, and other fissile components were produced when ^{238}U was transmuted to higher actinides particularly ^{239}Pu and ^{241}Pu. The cumulative effect was that the production of ^{239}Pu and ^{241}Pu levels increased towards the EOC [7]. On the other hand, in MOX core the fissionable materials originally in the core were ^{235}U and ^{239}Pu, so the ^{239}Pu amount gradually increased due to the transmutation of ^{238}U to ^{239}Pu plus the original amount found. As time passed, ^{239}Pu amount decreased due to fission; that was why the ^{239}Pu increased then decreased in fig. 11.

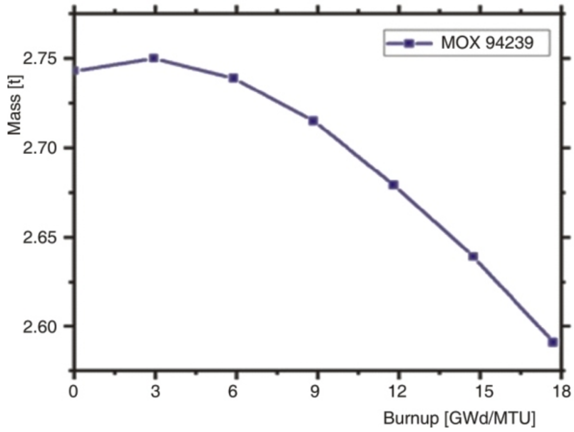

Figure 11. Consummation of ^{239}Pu in MOX with burnup

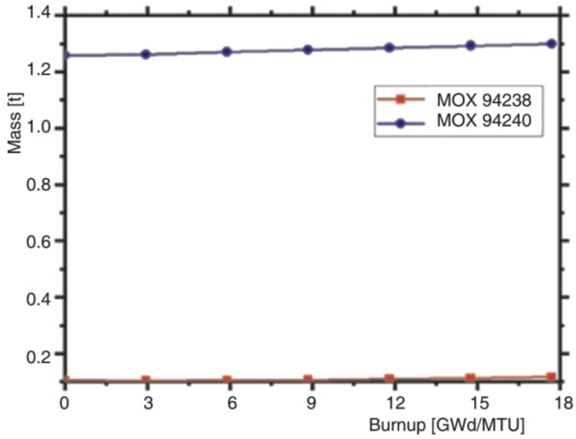

Figure 12. Production of higher isotopes in MOX with burnup

Figure 13 shows the MOX core power distribution in unit of MW. The power peaking factor was found to be 1.855 and 1.979 for UO_2 and MOX cores respectively.

The variation between the results of two libraries, the ENDF/B-VII.1 and the ENDF/B-VIII, was

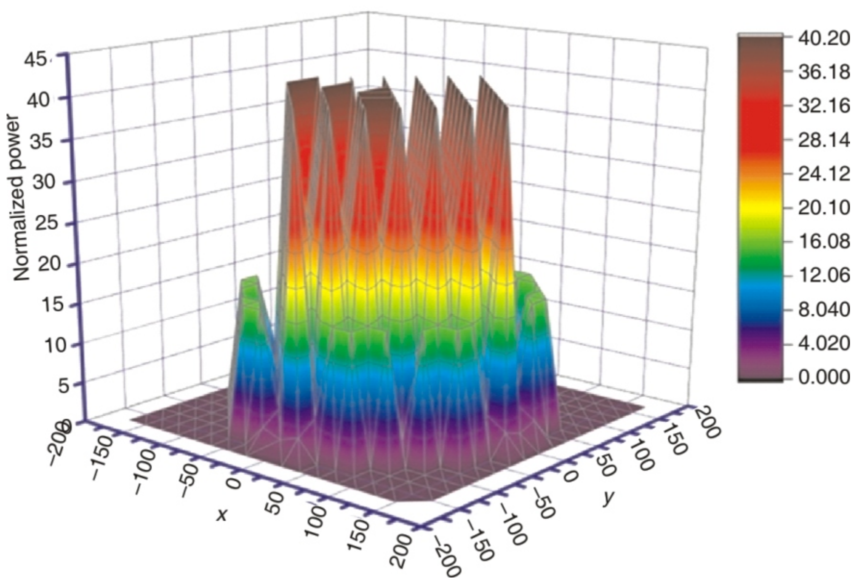

Figure 10. Core power distribution for UO_2 reactor (MW)

Figure 13. Core power distribution for MOX reactor (MW)

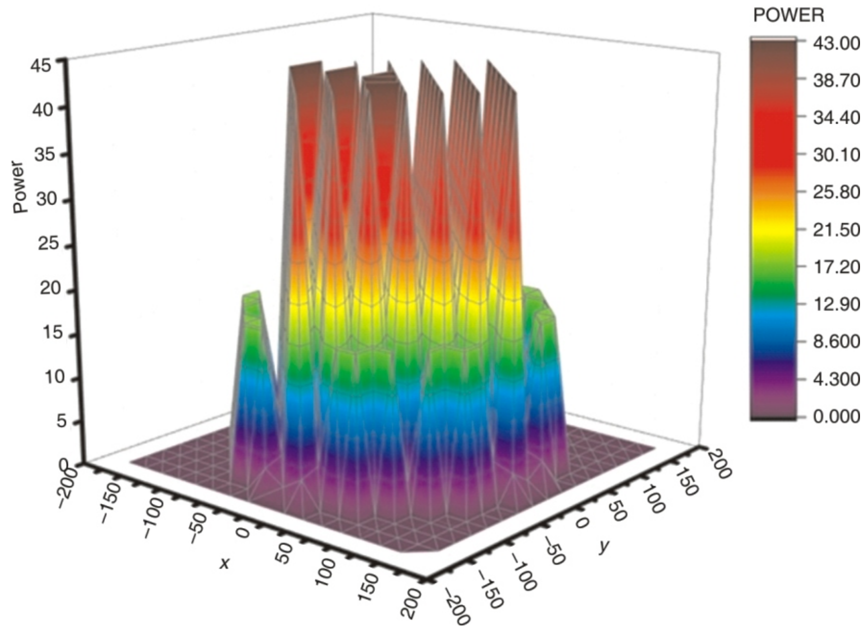

small. The consummations and productions of MOX fuel are shown in tab. 7. It shows that the variations occurred in the isotope mass in tons for all MOX fuel compositions.

The fuel used in MOX assemblies was characterized by a reduced enrichment in uranium, which was depleted and by a content of weapons-grade and other reactor-grade plutonium. The higher values of thermal fission and absorption cross-sections of ^{239}Pu had two important effects:

– The thermal flux in MOX assemblies was lower than in LEU assemblies [18].
– The pins located at MOX/UO_2 interfaces presented a severe power peaking [18].

The first effect deserves a better description. The thermal neutron flux in MOX assemblies is substantially lower than in LEU ones and also the fast flux is slightly smaller. This means that the burnup for UO_2 fuel will be faster than that of MOX as shown in fig. 6.

The fast-to-thermal ratio in MOX is almost twice that of UO_2. These facts lead to some particular phenomena. One of the most important phenomena is the reduction in reactivity value of neutron-adsorbing materials. The effectiveness of boric acid (H_3BO_3) that is used to offset the burnup of the fuel and of the burnable absorber, is reduced since it is a thermal absorber [16, 17].

One of the most important parameters is the effective delayed neutron fraction β_{eff}. If β_{eff} has a lower value, more neutrons appear as prompt neutrons. Therefore, the kinetic response of the reactor is quicker. ^{239}Pu has a delayed neutron fraction that is significantly smaller than ^{235}U. MOX cores also respond more quickly than UO_2 cores, tab. 5.

Table 7. The burnup of MOX fuel with the ENDF/B-VII.1 and the ENDF/B-VIII

	92235		92238		95241	
Time	ENDF/B-7	ENDF/B-8	ENDF/B-7	ENDF/B-8	ENDF/B-7	ENDF/B-8
0	2.355	2.355	79.20	79.20	0.1228	0.1228
100	2.298	2.299	79.15	79.15	0.1258	0.1255
200	2.243	2.243	79.10	79.10	0.1286	0.1281
300	2.189	2.189	79.05	79.05	0.1314	0.1306
400	2.137	2.136	78.99	79.0	0.1341	0.133
500	2.086	2.086	78.94	78.94	0.1367	0.1353
600	2.035	2.036	78.89	78.89	0.1392	0.1375
	94238		94239		94240	
Time	ENDF/B-7	ENDF/B-8	ENDF/B-7	ENDF/B-8	ENDF/B-7	ENDF/B-8
0	0.09552	0.09552	2.479	2.479	1.137	1.137
100	0.09498	0.09509	2.48	2.479	1.138	1.138
200	0.09498	0.09527	2.48	2.479	1.139	1.139
300	0.09534	0.09583	2.478	2.476	1.14	1.141
400	0.09596	0.09668	2.475	2.473	1.141	1.142
500	0.09676	0.09773	2.471	2.467	1.143	1.144
600	0.09771	0.09894	2.466	2.461	1.145	1.146

The MOX fuel results in a slightly larger Doppler coefficient and a significantly larger moderator temperature coefficient is shown in tab. 6. This condition can be considered in accident scenarios characterized by the overcooling of the core; the overcooling of MOX fuel will result in a larger increase in reactivity than that of UO_2 fuel [18].

CONCLUSION

In this investigation, the AP1000 reactor core was modeled by using the MCNP6 code. The model was validated by comparing with the design control document (DCD) of the AP1000 and the published data. The simulation results of the current study, including core reactivity, cold zero power (CZP) neutronic parameters, temperature reactivity coefficients, core power distribution, neutron flux, core reactivity *vs*. fuel burnup and power peaking factor were in good agreement with the DCD. The multiplication factor k_{eff} was found to be 1.20495 compared to 1.205 for the AP1000 DCD. The delayed neutron fraction β_{eff} was found to be 0.00676 compared to 0.0075 for the AP1000 DCD. The temperature reactivity coefficients have also demonstrated values close to those in DCD. The distribution of fuel burn-up and content of transuranic nuclides produced in the AP1000 core were successfully calculated and the analysis showed a consistent result compared to reference data. The production of TRU and fuel consumption showed also a good agreement with DCD. The results showed the accuracy of the MCNP6 code in calculating the reactor power in addition to establishing a precise evaluation of the neutronics parameters by means of the two ENDF/B-VII.1 and ENDF/B-VIII libraries. A new core with MOX fuel was analyzed keeping the fuel assembly geometry. The multiplication factor k_{eff} was found to be 1.19988 which meant that it was in the reasonable area. The delayed neutron fraction β_{eff} was found to be 0.0052. This was because the ^{239}Pu had a delayed neutron fraction which was significantly smaller than ^{235}U. The temperature reactivity coefficients for MOX fuel were slightly higher than those for UO_2 fuels.

AUTHORS' CONTRIBUTIONS

S. M. Reda and I. M. Gomaa shared the presented idea carried out the calculations, and wrote the manuscript. All authros discussed the results and contributed to the final version of the manuscript.

REFERENCES

[1] Wenchao Hua, *et al*., Minor Actinide Transmutation on PWR Burnable Poison Rods, *Annals of Nuclear Energy, 77* (2015), March, pp. 74-82

[2] Schulz, T., Westinghouse AP1000 Advanced Passive Plant, *Nuclear Engineering and Design, 236* (2006), 14-16, pp. 1547-1557

[3] Rendong Jia Bin Liu, *et al*., Minor Actinide Transmutation Characteristics in AP1000, *Annals of Nuclear Energy, 115* (2018), May, pp. 116-125

[4] ***, Westinghouse, AP1000 Design Control Document Rev. 19, June 21, 2011

[5] Robert, J., AP1000 Core Design with 50 % MOX loading, *Annals of Nuclear Energy, 36* (2009), 3, pp. 324-330

[6] Washington, J., King, J., Optimization of Plutonium and Minor Actinide Transmutation in an AP1000 fuel Assembly Via a Genetic Search Algorithm, *Nuclear Engineering and Design, 311* (2017), Jan., pp. 199-212

[7] Ames, II D., High-Fidelity Nuclear Energy System Optimization Towards an Environmentally Benign, Sustainable and Secure Energy Source, PhD Thesis, Texas A&M University, 2010

[8] ***, Nuclear Energy Agency, NEA No. 6224 Very High Burn-ups in Light Water Reactors, Organization for Economic Co-Operation and Development, *Nuclear Science Committee*, ISBN 92-64-02303-8, 2006

[9] ***, Status and Advances in MOX Fuel Technology, International Atomic Energy Agency, Vienna, Technical Reports Series No. 010/415, 2003

[10] Pelowitz, B., MCNP6TM USER'S MANUAL, Version 1.0, Manual Rev. 0, LA-CP-13-00634, Rev. 0, May, 2013

[11] Conlin, J., *et al*., Release of ENDF/B-VIII.0-Based ACE Data Files, Nuclear Data Team, XCP-5, Los Alamos National Laboratory, LA-UR-18-24034, May 23, 2018

[12] Capote, R., *et al*., IAEA CIELO Evaluation of Neutron-Induced Reactions on ^{235}U and ^{238}U Targets for Incident Energies up to 30 MeV, *Nuclear Data Sheets 148* (2018), 25

[13] Brown, D. A., *et al*., ENDF/B-VIII.0: The 8$^{\text{th}}$ Major Release of the Nuclear Reaction Data Library with CIELO-project Cross Sections, New Standards and Thermal Scattering Data. In: Nuclear Data Sheets 148, Special Issue on Nuclear Reaction Data, pp. 1-142, issn: 0090-3752, 2018

[14] Chadwick, M., *et al*., CIELO Collaboration Summary Results: International Evaluations of Neutron Reactions on Uranium, Plutonium, Iron, Oxygen and Hydrogen, *Nuclear Data Sheets,* (2018), pp. 148-189

[15] Elsawi, A., Bin Hraiz A., Benchmarking of the WIMS9/PARCS/TRACE Code System for Neutronic Calculations of the Westinghouse AP1000TM Reactor, *Nuclear Engineering and Design, 293* (2015), Nov., pp. 249-257

[16] Maiorino, J. R., Stefani, G. L., Utilization of Horium in PWR Reactors – First Step Toward a Th-U Fuel Cycles, 26$^{\text{th}}$ International Conference Nuclear Energy for New Europe, Bled Slovenia, 2017

[17] Stefani, G. L., *et al*., Detailed Neutronic Calculations of the AP1000 Reactor Core with the Serpent Code, *Progress in Nuclear Energy, 116* (2019), Sept., pp. 95-107

[18] Venturini, A., Neutronic Investigations of MOX and LEU Fuel Assemblies for VVER Reactors, Universita de glistudi di Pisa, 2013/2014

[19] Sembiring, T. M., *et al*., Evaluation of the AP1000 Delayed Neutron Parameters Using MCNP6, Journal of Physics: Conference Series, Conf. Ser. 962 012030, 2018

[20] Compton, W., Impact of Configuration Variations on Small Modular Reactor Core Performance, M.Sc., thesis, Missouri University of Science and Technology, 2015

Received on July 5, 2019
Accepted on December 31, 2019

Сониа М. РЕДА, Ибрахим М. ГОМА, Ибрахим И. БАШТЕР, Есмат А. АМИН

УТИЦАЈ MOX ГОРИВА И ENDF/B-VIII БИБЛИОТЕКЕ НА ИЗРАЧУНАВАЊЕ НЕУТРОНСКИХ ПАРАМЕТАРА AP1000 РЕКАТОРА ПОМОЋУ MCNP6 ПРОГРАМА

Проучаван је утицај увођења MOX горива на неутронске параметре Вестинхаусовог AP1000 реактора. Неутронска израчунавања језгра реактора AP1000 са три зоне обогаћења ^{235}U (2.35 %, 3.40 %, и 4.55 %) извршена су употребом MCNP6 кода са библиотеком ENDF/B-VII.1 и новим издањем ENDF/V-VIII. Добијени резултати показали су да симулирани модел језгра AP1000 реактора задовољава критеријуме оптимизације као у Вестингхаусовој референци. Резултати који су укључивали: ефективни фактор умножавања $k_{\rm eff}$, фракцију закаснелих неутрона $\beta_{\rm eff}$, вишак реактивности $\rho_{\rm ex}$, границу заустављења, температурне коефицијенте реактивности, потрошњу целог језгра, неутронски флукс, фактор максималне снаге и густину снаге језгра, израчунати су и упоређени са доступним објављеним подацима.

Утврђено је да је $k_{\rm eff}$ за хладан реактор нулте снаге 1.20495 и 1.20247, са библиотекама ENDF/B-VII.1 и ENDF/B-VIII, што одговара вредности од 1.205 представљеној у AP1000 контролном пројектном документу за језгро са горивом UO_2. С друге стране, утврђено је да $k_{\rm eff}$, под истим условима, износи 1. 19988 и 1.19860 за MOX језгро прорачунато коришћењем библиотека ENDF/B-VII.1 и ENDF/B-VIII, што показује добар одзив, потврђује сигурност пројекта и ефикасно моделовање језгра реактора AP1000.

Кључне речи: рекӣор AP1000, MOX ȳориво, неуӣронски ӣарамеӣри, MCNP6, ENDF/B-VIII